Toxicology Letters 221 (2013) 91–101

Contents lists available at SciVerse ScienceDirect

Toxicology Letters

journal homepage: www.elsevier.com/locate/toxlet

Testicular phosphoproteome in perfluorododecanoic acid-exposed rats

Zhimin Shi[a,1], Junjie Hou[b,1], Xuejiang Guo[c], Hongxia Zhang[a], Fuquan Yang[b,**], Jiayin Dai[a,*]

[a] Key Laboratory of Animal Ecology and Conservation Biology, Institute of Zoology, Chinese Academy of Sciences, Beijing 100101, PR China
[b] Laboratory of Proteomics, Institute of Biophysics, Chinese Academy of Sciences, Beijing 100101, China
[c] State Key Laboratory of Reproductive Medicine, Department of Histology and Embryology, Nanjing Medical University, Nanjing 210029, PR China

HIGHLIGHTS

- A total of 4077 unique phosphopeptides from 1777 proteins were identified.
- 937 unique phosphorylation sites were considered to be novel in testicular proteins.
- MAPK pathway and CDC2 protein phosphorylation are critical for PFDoA toxicity.

ARTICLE INFO

Article history:
Received 14 April 2013
Received in revised form 12 June 2013
Accepted 13 June 2013
Available online 22 June 2013

Keywords:
Testes
Phosphoproteome
MAPK
CDC2
PFDoA

ABSTRACT

Perfluorododecanoic acid (PFDoA) is a common environmental pollutant, which has been detected in human sera and has adverse effects on testicular function in animal models. Exploring phosphorylation events in testes helps elucidate the specific phosphorylation signals involved in testicular toxicity of PFDoA. Combining efficient prefractionation of tryptic peptide mixtures using self-packed reversed phase C18 columns with TiO_2 and IMAC phosphopeptide enrichment techniques followed by 2D-LC–MS/MS, we identified 4077 unique phosphopeptides from 1777 proteins with a false discovery rate below 1.0% in the testes of rats exposed to PFDoA for 110 days. In addition, 937 novel phosphorylation sites were discovered in testicular proteins. Hundreds of phosphorylated proteins identified might be involved in spermatogenesis and sperm function. With increasing PFDoA dosage, the number of casein kinase 2 kinase-modified peptides significantly increased. Pathway analysis suggested that the mitogen-activated protein kinase pathway and cell division cycle protein 2 (CDC2) may have contributed to sperm activity and testicular function. By *in vitro* experiments, CDC2 phosphorylation activity was found to be likely involved in PFDoA-induced toxicity in Leydig cells. This study provides the first examination of the whole proteins' phosphorylation profile in rat testis and suggests that the MAPK pathway and CDC2 protein phosphorylation are critical for PFDoA testicular toxicity.

1. Introduction

Male testes are responsible for spermatogenesis, which is enabled by testosterone produced in the Leydig cells. Testicular functions are regulated by complex signals at the genetic and protein levels, such as the post-translational modification of proteins. Phosphorylation by protein kinases is the most widespread post-translational modification used in signal transduction and regulates many biological processes (Urner and Sakkas, 2003). Global identification of *in vivo* phosphorylation is essential for a thorough and therapeutically applicable understanding of cellular functions during physiological and pathological states. Phosphoproteomics aims to map the phosphorylation status of proteomes in a high-throughput manner, discover new phosphorylation sites, and ultimately improve understanding of biological function regulation mediated by phosphorylation (Hojlund et al., 2009). Several protein kinases are involved in testicular functions such as steroidogenesis and spermatogenesis. The cAMP-PKA pathway and protein phosphorylation perform crucial roles in steroid hormone synthesis in the testis (Andric et al., 2007; Evaul and Hammes, 2008). For example, PKA-induced phosphorylation of

Abbreviations: PFAAs, perfluoroalkyl acids; PFDoA, perfluorododecanoic acid; TiO_2, titanium dioxide; IMAC, immobilized metal affinity chromatography; MAPK, mitogen-activated protein kinase; TSSK, testis-specific serine/threonine kinases; ODF, outer dense fiber protein; CDC2, cell division cycle protein 2.

* Corresponding author. Tel.: +86 10 64807185.
** Corresponding author. Tel.: +86 10 66888581.
E-mail addresses: fqyang@sun5.ibp.ac.cn (F. Yang), daijy@ioz.ac.cn (J. Dai).

[1] These authors contributed equally to this paper.

0378-4274/$ – see front matter © 2013 Elsevier Ireland Ltd. All rights reserved.
http://dx.doi.org/10.1016/j.toxlet.2013.06.219

steroidogenic acute regulatory protein (StAR) is essential for producing progesterone and testosterone in Leydig cells. Sperm phosphoproteomics studies have provided important insights into sperm activity and related diseases (Ficarro et al., 2003). Although many studies have been published on phosphorylation events in testes, detailed mechanisms of protein phosphorylation and the related significance to testicular function are poorly understood.

Testicular diseases and abnormal reproduction are serious issues in the general population. Numerous studies have suggested that testes are potential target organs for various environmental pollutants such as man-made perfluoroalkyl acids (PFAAs), which are of global concern due to their widespread application in cosmetics, lubricants, fire retardants, and insecticides (Kennedy et al., 2004). These chemicals consist of a series of compounds with different carbon chain lengths, including perfluorododecanoic acid (PFDoA, C12), perfluorodecanoic acid (PFDA, C10), and perfluorooctanoic acid (PFOA, C8). Because of the high energy C—F bond, PFAAs are difficult to degrade and therefore persist in water, soil, wildlife, and humans (Kennedy et al., 2004; Tao et al., 2008; Van de Vijver et al., 2007). For example, PFDoA has been detected in human breast milk and sera and in the livers of harbor porpoises, with the highest detected concentrations reaching 9.74 pg/ml, 0.022 ng/ml, and 9.5 ng/g (wet weight), respectively (Kennedy et al., 2004; Tao et al., 2008; Guruge et al., 2005). Animal experiments have demonstrated that PFDoA is the most toxic among the 8–12 carbon chain PFAAs (Kennedy et al., 2004) and its potential risk to the environment and human populations has been raised among environmental agencies and toxicologists. In our previous studies, we observed that chronic PFDoA exposure disrupted testicular steroid production and testicular structure in rats (Shi et al., 2009). In addition, our proteomic study on PFDoA-treated rat testes showed that the toxic effects of PFDoA were related to oxidative stress and mitochondrial disruption in testes (Shi et al., 2010a). However, the detailed molecular mechanism by which PFDoA leads to testicular toxicity in rats remains unclear.

Combining efficient prefractionation of tryptic peptide mixtures using self-packed reversed phase C18 columns with titanium dioxide (TiO_2) and immobilized metal affinity chromatography (IMAC) phosphopeptide enrichment techniques, along with two-dimensional liquid chromatography tandem mass spectrometry (2D-LC MS/MS), we analyzed the phosphoproteome of normal rat testes and testes after 110 days of PFDoA exposure. We aimed to clarify global phosphorylation profiles and explore the key phosphorylation events in normal testicular function. Comparing the testicular phosphorylation profiles between normal and PFDoA-treated rats will help determine the molecular mechanism of the toxic action of PFDoA in testes at the protein phosphorylation level.

2. Materials and methods

2.1. Animal treatment

Male Sprague-Dawley rats (40–50 g) were obtained from the Weitong Lihua Experimenter Animal Center, Beijing, China. Animals were randomly classified by body weight into treatment and control groups (six rats per group), and were individually housed and maintained in a mass air-displacement room with a 12-h light-dark cycle at 20–26 °C and a relative humidity of 50–70%. Animals had access to food and water *ad libitum*. The PFDoA (95% purity; Sigma–Aldrich, St. Louis, MO) was dissolved in 0.2% Tween-20. The treated rats were daily gavaged for 110 days with PFDoA doses of 0.02, 0.2, or 0.5 mg/kg/d. The control rats were similarly treated with 0.2% Tween-20 only. At the end of the experimental period, all rats were euthanized by decapitation. Testes were immediately isolated and frozen in liquid nitrogen and stored at −80 °C for further analysis.

2.2. Protein extract, tryptic digestion and peptide prefractionation

Details of protein extract and tryptic digestion are given in supporting information. The peptide prefractionation has been described previously (Hou et al., 2010). Briefly, an individual sample was loaded sequentially onto three self-packed C18 columns (40–60 μm, 120-Å pore size, SunChrom, Friedrichsdorf, Germany). The final fractions eluted from the three columns using the same elution buffer were combined, divided into two equal parts, and dried with a speed vac. One dried sample was used for subsequent TiO_2 enrichment, and the other was used for IMAC enrichment.

2.3. Phosphopeptide enrichment with TiO_2 and IMAC and 2D-nano LC–MS/MS analysis

Phosphopeptide enrichment was carried out using TiO_2 and IMAC with slight modifications and details of them are given in supporting information (Wu et al., 2007). Finally, all fractions from the same treatment were combined, dried, and stored at −80 °C until 2D-LC–MS/MS analysis.

Analysis was performed as previously described (Hou et al., 2010; Cui et al., 2009). Details of analysis are given in supporting information. The application of mass spectrometer scan functions and HPLC solvent gradients were controlled by an XCalibur data system (Thermo Fisher Scientific). The MS analysis was performed twice for each set of pooled samples.

2.4. MS data processing

Raw MS data were processed using Bioworks 3.3 (Thermo Fisher Scientific Inc.) with the following parameters: mass range, 450–5500; precursor tolerance, 1.4 amu; ion counts, 10; intensity threshold, 1000 (absolute). Bioworks-generated peak lists (.dta files) were searched against the rat International Protein Index (IPI) database version 3.51 (40,288 protein entries) and its random sequences with SEQUEST v.28 (rev. 12) (Eng et al., 1994). Parameters of the database search were as follows: full tryptic specificity, 2.0 Da for a precursor ion mass tolerance, 0.8 Da for fragment ion mass tolerance, Cys carboxyamidomethylation (57.02 Da) as fixed modification, two missed cleavage sites, Ser, Thr, and Tyr residue phosphorylation (79.96 Da), and Met residue oxidation (15.99 Da) as the dynamic modifications. Each peptide was allowed three phosphorylation sites.

Phosphopeptide hits were filtered by Rsp, Sf, DeltaCn', and Xcorr' scores (Hou et al., 2010). The Rsp is the preliminary score rank for each peptide based on the SEQUEST algorithm. In our study, we chose Rsp ≥ 2. The Sf score (0–1.0) for each phosphopeptide created by the Bioworks program was calculated using a neural network algorithm that incorporated the Xcorr, DeltaCn, Sp, RSp, peptide mass, charge state, and the number of matched peptides for the search. The XCorr' was calculated using the following formula: $XCorr' = \ln(XCorr)/\ln(L)$. In this formula, L stands for peptide length. The DeltaCn' was defined as the normalized difference between the XCorr values of the top hit and the next hit with a different amino acid sequence, calculated with an in-house Perl program. The DeltaCn' of each peptide should be ≥0.1; for peptides with a charge of +2, the Xcorr' value should be ≥0.25, and for peptides with a charge of >+3, the Xcorr' value should be ≥0.35. The false-discovery rate (FDR) was calculated as the number of decoy-hits divided by the number of target-hits, with the threshold of the Sf value (not less than 0.4) adjusted to fit a final FDR of ≤0.01. After filtering, the lowest Xcorr values in the dataset were 1.565, 2.024, 2.022, and 2.056 for groups one to four, respectively.

The ambiguity scores (Ascore) of each phosphorylation site were calculated using software developed by Beausoleil et al. (2006). Only phosphorylated sites with Ascores above 19 were considered reliable ($p \leq 0.01$).

2.5. Bioinformatics analysis

Specific motifs were obtained from the data set with the Motif-X algorithm (Schwartz and Gygi, 2005). All single phosphorylation sites with an Ascore value above 19 were used for motif analysis. NetworKIN-2.0 was used to predict probable kinase families and identify phosphorylation sites (Linding et al., 2008). All phosphorylated sites with an Ascore value ≥19 were utilized for this analysis, kinase-substrate relationships with a NetworKIN score above 1.0 and a String score above 0.6 were regarded as significant. When one specific phosphorylation site was predicted to be potentially recognized by multiple kinases, the one with the highest NetworKIN Score was retained.

Gene ontology data analysis was carried out with Cytoscape and Plugin BiNGO (Maere et al., 2005). We compared the annotations of phosphorylated proteins with those of the entire *Rattus norvegicus* proteome. The hypergeometric statistical test and the multiple-test Benjamini and Hochberg FDR correction were adopted to derive over-represented functions. The level of significance was set as $p < 0.05$.

Analysis of the relationship between identified phosphorylated proteins in rat testes was performed with text-mining Pathway Studio™ (v7.0) software (Ariadne Genomics, Inc., Rockville, MD), which uses a database assembled from scientific abstracts and a manually created dictionary of synonyms to recognize biological terms. The phosphorylated proteins were converted to their corresponding gene IDs and imported into Pathway Studio software; each identified relationship was confirmed manually with the relevant PubMed/Medline hyperlinked texts.

For novel phosphorylated sites analysis, the phosphorylated peptides (Ascore value ≥19) were first searched against rat data from UniProt to filter the known sites (http://www.uniprot.org). The filtered peptides were then manually compared to mouse and human phosphorylated sites in phosphoSitePlus (http://www.phosphosite.org) to obtain the novel sites.

2.6. Primary Leydig cell culture

Isolation of rat Leydig cells was performed as previously described (Mondillo et al., 2009). Briefly, freshly harvested testes obtained from six adult Sprague-Dawley (SD) rats were decapsulated and dispersed by collagenase dissociation (0.5 mg/ml). Leydig cells were further purified by discontinuous Percoll (GE Healthcare Bio-Sciences, Uppsala, Sweden) gradient (density range 1.01–1.126 g/l) centrifugation at 800 × *g* for 30 min. The preparations contained 70–80% Leydig cells, as determined by histochemical staining for 3β-HSD (Klinefelter et al., 1987). Leydig cells were cultured for 24 h with PFDoA (1–100 μM), as described previously (Shi et al., 2010b). Following incubation, the cells were stimulated for 3 h with 1 mM of cAMP in serum-free medium. Cells were used for immunohistochemistry staining analysis with corresponding antibodies and mitochondrial H_2O_2 determination.

2.7. Phosphopeptide validation, Western blot, immunohistochemistry and mitochondrial membrane potential measurement

Three synthesized phosphopeptides (AFSpEPVLSEPMFSEGEIK, FKVESpFR, and PMSpPPVPK, where p indicates phosphorylation site) with purity >98% (Scilight Biotechnology, Beijing, China) were analyzed by LC–MS/MS as described above. The MS/MS spectra of the synthesized peptides were then compared with those peptides identified in this study.

Protein samples extracted for tryptic digestion were used for Western blot analysis to validate the results of the 2D-nano LC–MS/MS analysis. For *in vitro* cell samples, cells were harvested and lysed by the same lysis buffer as phosphorylation peptide preparation. Details of Western blot analysis are given in supporting information.

Mitochondrial membrane potential was measured using tetramethylrhodamine methyl ester (TMRM) fluorescent dye (Adinolfi et al., 2005). Briefly, the dye was loaded onto cells at 150 nM in assay buffer (80 mM of NaCl, 75 mM of KCl, 25 mM of D-glucose, 25 mM of HEPES, pH 7.4) at 37 °C for 5 min, washed four times in PBS, and measured on a FLUOstar Omega microplate reader (Excitation: 544 nm and Emission: 590 nm, bottom reading with 50 flashes per well).

3. Results

3.1. Testicular phosphorylation profiles in rats

Rats were exposed to three different PFDoA doses (0.02 (low), 0.2 (medium), or 0.5 mg/kg/d (high)). Protein was extracted from the testis of all rat individuals, then the six samples from each group were randomly divided into two groups of three. Equal amounts of protein from each subsequent group were pooled to yield two protein samples. These samples were analyzed *via* off-line RP fractionation, followed by two different phosphopeptide enrichments. The resulting 16 (8 × 2) phosphopeptide mixtures were subjected to on-line 2D-LC (SCX/RP)-MS/MS analysis. The collected MS/MS data were searched against the combined target-decoy rat IPI database with the SEQUEST algorithm (Eng et al., 1994). As shown in Table 1, 9099, 4753, 5075, and 6784 phosphorylated peptides were identified after rats were given 0, 0.02, 0.2, and 0.5 mg/kg/d PFDoA, respectively, of which 1519, 1161, 1538, and 1801 peptides were unique. After combining results from the four groups, 22,678 phosphopeptides with FDR below 1% were obtained, which represented 4077 unique phosphopeptides from 1777 proteins (Table 1). In addition, 933, 641, 864, and 957 unique proteins were identified following administration of 0, 0.02, 0.2, and 0.5 mg/kg/d PFDoA, respectively (Table 1). Further analysis showed that 212 proteins were common across all groups (Fig. 1A). All MS/MS spectra of the unique phosphopeptides in the control group are provided as supplementary material (Fig. S1) and the peak list for all groups can be accessed in supporting information (Table S1). When either the peptide sequence was different or the peptide sequence was the same but with different phosphorylated site(s), as evaluated by the Ascore algorithm, we considered the phosphopeptide as a unique peptide. In control group, about 89.9% of the phosphopeptides were singly phosphorylated, while doubly and triply phosphorylated peptides accounted for 6.3% and 3.8%, respectively (Table S2). The distribution of phosphoserine (pS), phosphothreonine (pT), and phosphotyrosine (pY) residues in control group (with an Ascore value ≥19) was roughly 86:12:1 (Table S2), similar to previous research (86.4:11.8:1.8) (Olsen et al., 2006). The characteristics of phosphorylated proteins in rat testes treated by PFDoA were given in supplementary data (Table S2).

Table 1
Summary of the characteristics of phosphorylated proteins in rat testes.

	Peptides	Unique peptides	Unique proteins
Total[a]	22,678	4077	1777
0 (PFDoA mg/kg/d)	9099	1519	933
0.02 (PFDoA mg/kg/d)	4753 (52%)[b]	1161 (76%)	641 (69%)
0.2 (PFDoA mg/kg/d)	5075 (56%)	1538 (101%)	864 (93%)
0.5 (PFDoA mg/kg/d)	6784 (75%)	1801 (119%)	957 (101%)

[a] Represents total number without overlapping across all groups.
[b] The numbers in parenthesis = (the number of peptides, unique peptides and unique proteins in PFDoA treatment divided by its value for its corresponding control group) × 100).

With the 4077 unique phosphopeptides, a total of 937 phosphorylation sites were identified as novel in testicular protein s by retrieval of phosphorylation site (Ascore value ≥19) information from UniProt (http://www.uniprot.org) and phosphoSitePlus (http://www.phosphosite.org), with those sites highly homologous to humans and mice excluded (Fig. 1B, Table S3).

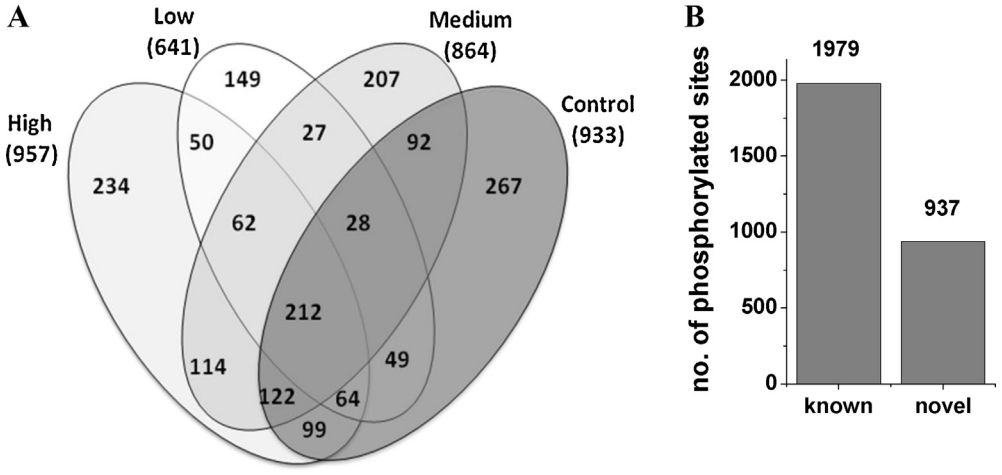

Fig. 1. Effects of PFDoA on phosphorylation of testicular proteins. (A) Venn diagram analysis of the phosphorylated proteins in normal and PFDoA-exposed rats. Numbers of phosphorylated proteins in the intersections are shown: $C \cap L = 353$, $C \cap M = 454$, $C \cap H = 497$, $L \cap M = 329$, $L \cap H = 388$, $M \cap H = 510$, $C \cap L \cap M = 240$, $C \cap L \cap H = 276$, $C \cap M \cap H = 334$, $L \cap M \cap H = 274$, $C \cap L \cap M \cap H = 212$. *C*, *L*, *M*, and *H* represent 0, 0.02, 0.2, and 0.5 mg/kg/d group, respectively. ∩ signifies overlapping. (B) Number of known phosphorylated sites and novel sites in all groups.

Comparison of the phosphorylation profiles between the control and PFDoA treatment groups showed that PFDoA at 0.02 mg/kg/d resulted in a reduction in total phosphorylated peptides, unique peptides, and unique proteins by 52%, 76%, and 69%, respectively, compared to the control group (Table 1). However, in other PFDoA treatment groups, PFDoA resulted in a reduction in total phosphorylated peptide by 56% and 75% at 0.2 and 0.5 mg/kg/d, respectively, compared to the control group. The profile for unique peptides and unique proteins between the control and other PFDoA treatment groups almost did not change. Our results suggest that PFDoA may affect testicular function at the post-translational level. However, no significant change in subcellular location occurred across the PFDoA-treated groups compared to the control group (Fig. S2A–D).

In addition, three phosphopeptides were randomly selected from our dataset (PMSpPPVPK, AFSpEPVLSEPMFSEGEIK, and FKVESpFR) and their observed MS/MS spectra were compared with the spectra obtained from the corresponding synthesized phosphopeptides. The results showed very high consistency between these spectra (Fig. S3). We also verified that the identified phosphorylated peptide PKIEDVGSpDEEDDSG was from HSP90β (phospho-Ser255) by Western blotting across all groups (Fig. S4). The results confirmed that our phosphoproteomic strategy was very efficient and our dataset was of high quality in representing the protein phosphorylation status in rat testes.

3.2. Effects of PFDoA on the motifs of phosphorylated peptides

In the control rats, three main motifs responsible for protein phosphorylation were identified by motif analysis. Proline-directed, basophilic, and acidic motifs represented 68.3%, 9.7%, and 3.8% of all motifs, respectively (Fig. 2A and Table S4). To determine the potential kinase(s) responsible for modification of the identified phosphosites, the phosphorylation motifs were annotated with NetworKIN (Table S4). The most abundant motifs were CDK2_CDK3 (38.7%), CK2 (11.8%), and p38 (4.8%) in normal rat testes (Fig. 2B). We predicted the relationships between kinases and all phosphorylation sites defined here to create the first kinase-substrate database for rat testes. This database was used to create an *in vivo* kinasome for the testis, comprising 38 kinases, representing most of the known kinase families.

As shown in Fig. 2A, acidic motifs accounted for 29.3%, 20.6%, and 28.9% of all motifs following administration of 0.02, 0.2, and 0.5 mg/kg/d PFDoA, respectively. Compared to the 3.8% acidic motif in the control rats, PFDoA administration resulted in a significant increase in this motif rate relative to other motifs. However, PFDoA did not significantly affect the percentage of proline-directed or basophilic motifs. The motif annotation showed that the most abundant motifs were from CDK2_CDK3 (40.5%), CK2 (30.2%) and p38 (4.0%) following administration of 0.02 mg/kg/d PFDoA, CDK2_CDK3 (37.1%), CK2 (29.1%), and p38 (5.1%) following administration of 0.2 mg/kg/d, and CDK2_CDK3 (30.6%), CK2 (41.9%), and p38 (3.6%), and following administration of 0.5 mg/kg/d PFDoA (Table S4). A key difference between the control and the PFDoA treatments was the CK2 motif (Fig. 2B). With increasing PFDoA doses, the peptides modified by the CK2 kinase increased significantly, suggesting that CK2 kinase may participate in the toxic effects of PFDoA in the testis.

3.3. Molecular function profile in control and PFDoA-exposed testis

The overall functional distribution of the identified phosphoproteins in control rats as determined by gene ontology (GO) analysis is shown in Table S5A. Most proposed functions involved cytoskeleton organization and biogenesis, male gamete generation, and spermatogenesis. The most abundant cellular components were

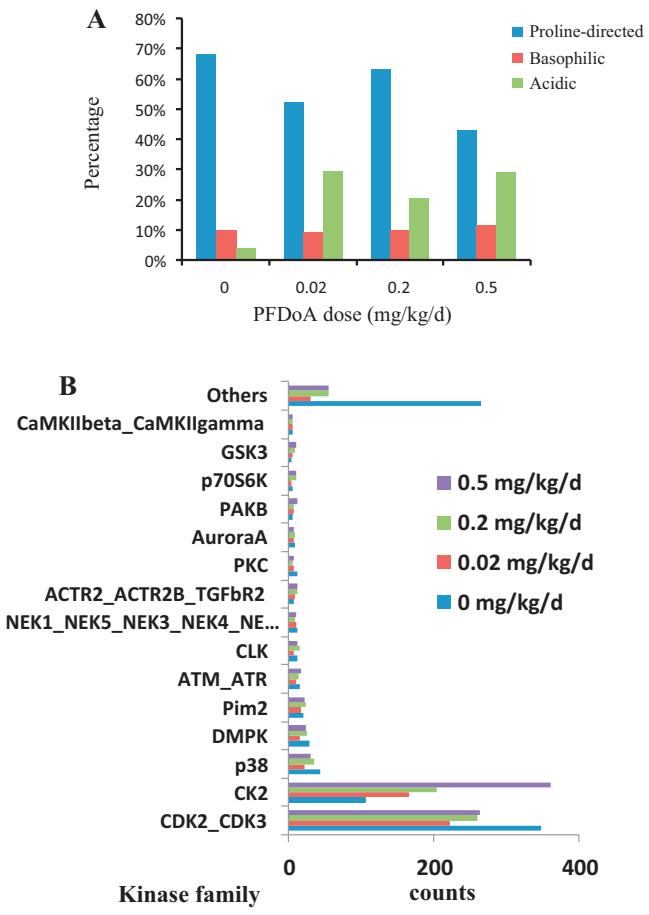

Fig. 2. Phosphorylation motif analysis and kinase prediction using testicular phosphoproteomic dataset. (A) Comparison of the different motifs that mediate protein phosphorylation. (B) All localized phosphorylation sites (Ascore value ≥19) were employed to predict the potential kinase families by use of NetworKIN 2.0. Protein kinase analysis.

intracellular and were localized in organelles and the nucleus. For the biological process category, a large proportion of the phosphoproteins were related to metabolism, organelle organization and biogenesis, reproduction, and development.

To further analyze the toxic mechanism of PFDoA, we integrated the phosphorylation profiles in PFDoA-exposed animals by comparing them to the control (Table S5B–D). Exposure to PFDoA resulted in changes in protein phosphorylation. For example, the protein kinase cascade and the peptidyl-serine phosphorylation process significantly decreased in PFDoA-treated rats. We also observed sperm activity-related alterations in the regulation of Ras protein signal transduction, cell cycle phase, and M phase in rats exposed to 0.02 mg/kg/d PFDoA (Table S5B). In addition, PFDoA exposure led to changes in other biological processes such as ribosome biogenesis, regulation of cellular protein metabolic processes, and actin filament organization (Table S5B). Cell component analysis showed that all doses of PFDoA may have caused alteration of proteins involved in the outer membranes of sperm, cell junctions, mitochondrial outer membranes, and microtubule-associated complexes (Table S5D). Further analysis demonstrated that cell junction proteins underwent a dose-dependent change after PFDoA exposure.

3.4. Pathway analysis in control rats

To analyze testicular signaling related to phosphorylated proteins, we performed pathway analysis of the identified proteins.

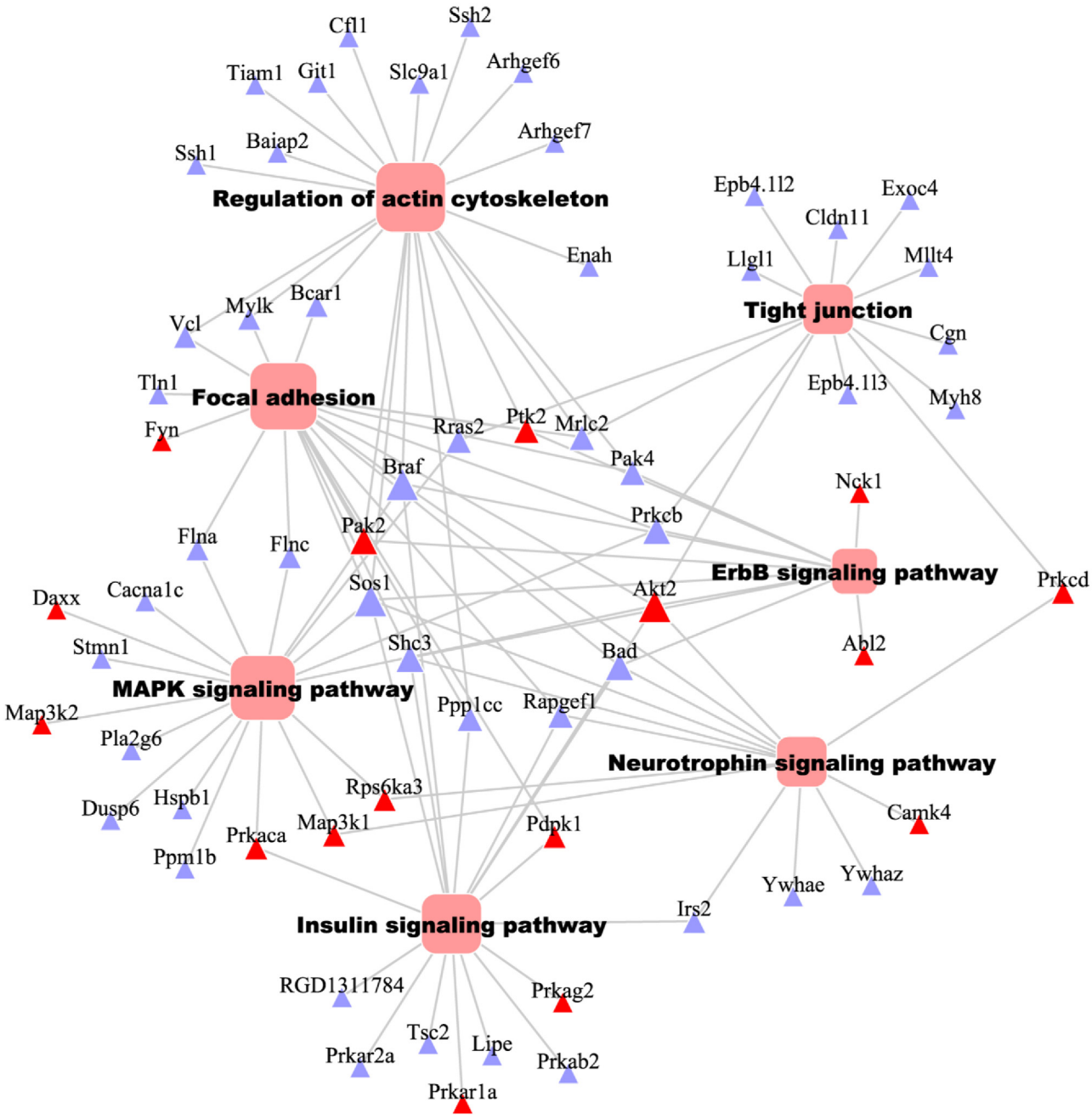

Fig. 3. Pathway analysis in normal rat testes based on phosphorylated proteins. The red triangle represents the kinase protein. The light blue triangle represents the non-kinase protein. (For interpretation of the references to color in this figure legend, the reader is referred to the web version of this article.)

The signaling pathways associated with phosphorylated proteins included the MAPK pathway, insulin signaling, tight junctions, the actin cytoskeleton, focal adhesion, and ErbB signaling (Fig. 3). Since the MAPK pathway plays a crucial role in testicular function (Almog and Naor, 2010), we further analyzed the regulatory network of this pathway. As the top regulator in this pathway, MAPK2 regulates a series of protein phosphorylation events such as CDC2 (Fig. S5). In addition to common regulatory proteins, we also identified potential proteins that may participate in the MAPK pathway *via* phosphorylation. For example, pathway analysis hinted that as a potential target stathmin may be phosphorylated by MAPK11 and MAPK13. Thus, future exploration of the mechanism of stathmin action on cellular skeleton organization is warranted.

We also performed interaction analysis on the identified phosphorylated proteins and composed the first network profile of protein phosphorylation in rat testes (Table S6). From this network, CDC2 may possibly interact with v-raf murine sarcoma viral oncogene homolog B1 (BRAF), which regulates MAPK signaling, providing useful information regarding the function of CDC2 in the MAPK pathway. We also explored the CDC2 network of protein regulation using Pathway Studio™ software (Fig. 4 and Table S7). These findings provide insight into the role of CDC2 in protein phosphorylation in the testis.

3.5. Changes in phosphorylation levels in PFDoA-exposed rats

To compare the degree of phosphorylation for specific phosphorylated peptides in one protein between the control and PFDoA-treated rats, we evaluated the relative phosphorylation levels of one protein with the same phosphorylation site across all

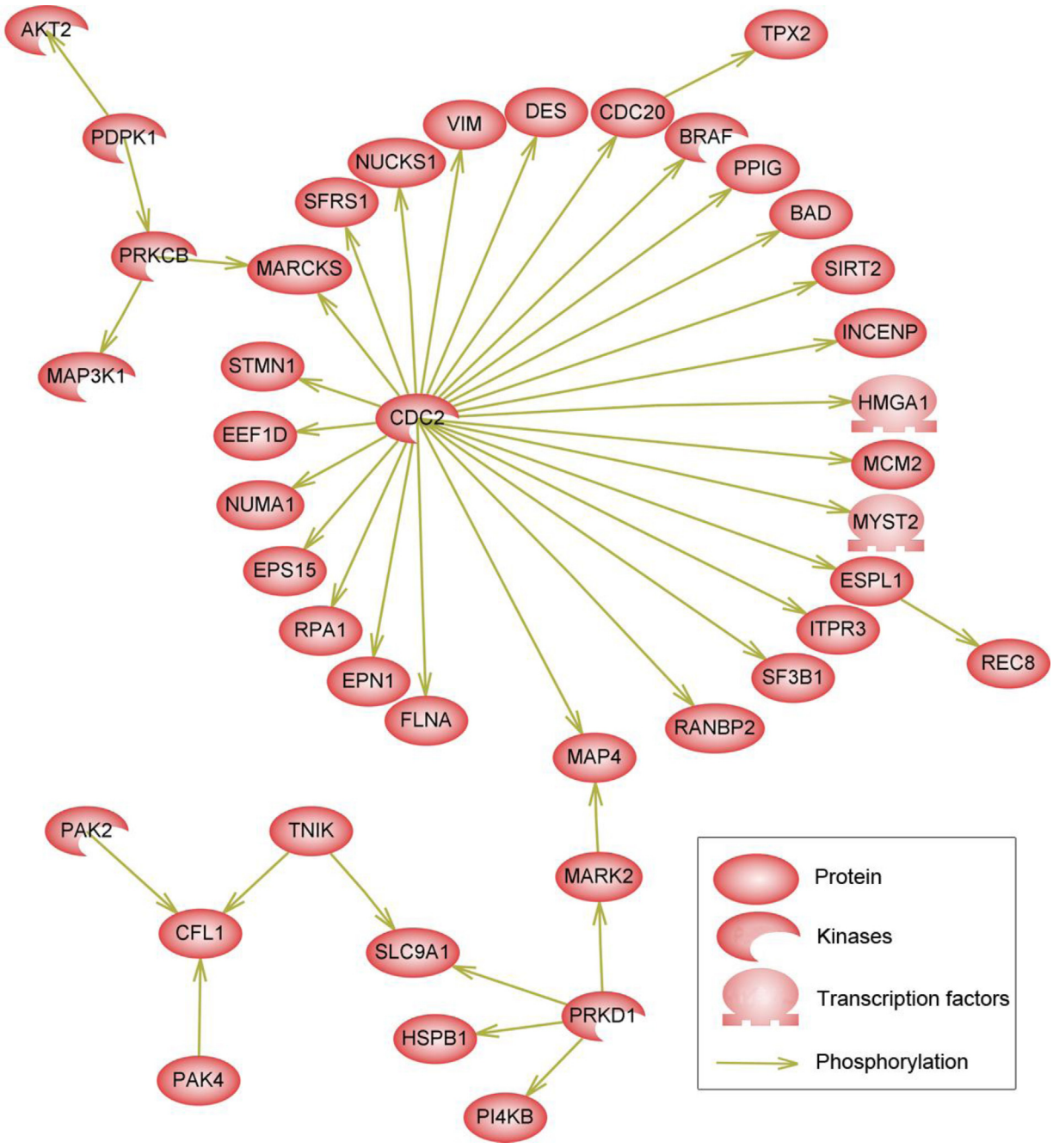

Fig. 4. Network of proteins that interact with CDC2 in rat testes (abbreviations for proteins are given in Table S7).

groups by calculating the MS2 spectral counts of each phosphopeptide. A three-fold difference in compared ratios was considered significant. We observed 214 phosphopeptides, corresponding to 152 proteins, in which the spectral counts significantly changed (Table S8). Not surprisingly, the phosphorylation levels at specific sites in most proteins exhibited significant decreases in the PFDoA-treated rats compared to the control. These phosphorylated proteins function in spermatogenesis, sperm activity, cytoskeleton regeneration, and oxidative stress (Table 2 and S8). For example, the phosphorylated peptide (ILASSCCSpSNILGSVNVCGFEPDQVK; Sp signifies phosphor-Ser) of outer dense fiber protein 1 (ODF1), which functions in sperm configuration and sperm motility, was 88, 21, 7, and 28 in 0, 0.02, 0.2, and 0.5 mg/kg/d exposure group, respectively. Proteins such as ODF1 (SpCGLCDLYYPCCLCDYK, ILASpSCCSpSpNILGSVNVCGFEPDQVK), which are phosphorylated at specific amino acids, only showed marked increases in the 0.5 mg/kg/d PFDoA group (high dose) compared to the control (Table 2 and S8). Interestingly, we also observed that phosphorylation at specific sites in some proteins only appeared in PFDoA-treated rats or controls, which implied that phosphorylation at different sites on the same protein, may exert various functions in PFDoA testicular toxicity. For example, the spectra counts of peptide RVS#VCAETFNPDEEEDNDPR from cAMP-dependent protein kinase type II-alpha regulatory subunit (PKAIIa) was high in the 0.02 mg/kg/d PFDoA group, while it was not detected in both the control group and 0.5 mg/kg/d exposure group. Our result from Western blot confirmed that the changes at the phosphorylation level of PKAIIa (Ser96) were high in the 0.02 mg/kg/d PFDoA group (Fig. 5). However, it is unclear if changes at the protein level contribute

Table 2
Phosphorylation levels of peptides involved in sperm function across all groups.

IPI accession number	Gene symbol	Protein description	Ascore peptide	Spectra counts/PFDoA (mg/kg/d)			
				0	0.02	0.2	0.5
IPI00734716.3	SPATA6	Spermatogenesis-associated protein 6	HVDPPSpPR	75	21	5	52
			ADNFFGSpPGR	52	2	2	44
			HCASpPVLNR	39	9	4	15
IPI00206296.2	ODF1	Outer dense fiber protein	ILASSCCSpSpNILGSVNVCGFEPDQVK	172	76	28	2
			ILASSCCSpSNILGSVNVCGFEPDQVK	88	21	7	28
IPI00464586.1	SPERT	Spermatid-associated protein	VQLSpDEMFVFQDGR	527	278	55	122
IPI00371167.2	PGM21L1	phosphoglucomutase 2-like 1	AVAGVMITASpHNR	98	34	19	4
IPI00209618.2	SAFB	Scaffold attachment factor B1	APTAAPSpPEPR	76	8	4	2
IPI00212365.1	AKAP4	A-kinase anchor protein 4	GYSpVGDLLQEVMK	46	60	2	24
IPI00201548.1	CARHSP1	Calcium-regulated heat stable protein 1	DRSpPSpPLRGNVVPSpPLPTR	44	2	16	2
IPI00201274.1	AKAP3	A kinase anchor protein 3	VIVSpNHNLADTVQNK	42	10	5	9
IPI00421390.1	KLHL10	Kelch-like protein 10	KMSpAMTCEIFNELR	36	2	9	5
IPI00230941.5	VIM	Vimentin	LLQDSpVDFSLADAINTEFK	36	1	1	1
IPI00201548.1	CARHSP1	Calcium-regulated heat stable protein 1	GNVVPSpPLPTR	29	2	17	8
IPI00231770.5	PRKAR1a	cAMP-dependent protein kinase type I-alpha regulatory subunit	EDEISpPPPPNPVVK	19	6	2	2
IPI00870825.2	MCM2	Minichromosome maintenance deficient 2 mitotin	ISDPLTSSpPGR	16	2	2	2
IPI00210923.1	PRM3	Protamine-3	LLLLEPEKQDGAEDAVAQPSpPEPK	13	2	20	12

to the changes at the phosphorylation level for other proteins.

In our previous study, we detected 40 proteins with significant changes from the same rats following PFDoA treatment by two-dimensional gel electrophoresis (2-DE) (Shi et al., 2010a). However, among these 40 proteins, we observed that only the stathmin phosphorylation level at Ser38 (SKESVPEFPLS*PPK) exhibited the same changing trend in protein levels after PFDoA exposure, suggesting PFDoA may produce toxic effects by disrupting protein phosphorylation levels directly.

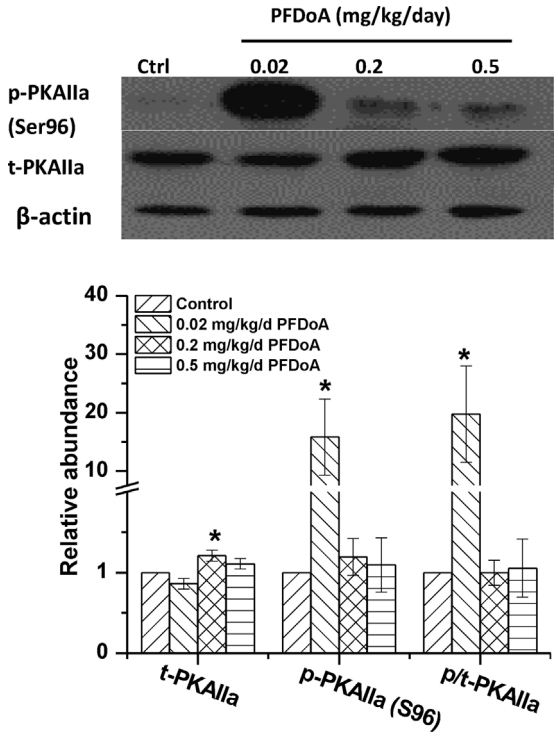

Fig. 5. Phosphorylated PKAIIa (Ser 96) and protein expression levels detected by Western blot, (upper) immunoblots of expression levels and phosphorylation levels of protein; (bottom) quantification of phosphorylated protein levels. Data are presented as means ± SEM ($n = 3$) from three independent experiments. * indicates significant difference from untreated controls ($p < 0.05$).

3.6. *Effect of PFDoA on primary Leydig cells and some proteins' phosphorylation in testes*

Based on the pathway analysis performed in the present study, we next focused on the role of CDC2 in PFDoA toxicity in the rat testis. Previous research has shown CDC2 to be a crucial molecule in mediating G2/M transition and cell apoptosis (Li et al., 2009). We tested whether CDC2 phosphorylation levels were inhibited by PFDoA in primary Leydig cells *in vitro*. In addition, previous study showed that oxidative stress, which is a major inducer of cell apoptosis, participated in the PFDoA-induced inhibition of testosterone (Yang et al., 2002). Thus, we examined the relationship of mitochondrial H_2O_2 levels with phosphorylation levels of AKT2 (phosphorylation at T451), PAK2 (phosphorylation at S141), and CDC2 (phosphorylation at Y15) following PFDoA exposure. Results showed that neither 1 mM of cAMP nor cAMP combined with PFDoA (1–100 μM) exhibited any observable effects on mitochondrial membrane potential of primary Leydig cells (Fig. 6A). However, 10 μM and 100 μM of PFDoA significantly increased mitochondrial H_2O_2 production (Fig. 6B).

By Western blot analysis, 1–100 μM of PFDoA exhibited marked inhibition for CDC2 phosphorylation at Y15. Both 10 μM and 100 μM of PFDoA significantly inhibited AKT2 phosphorylation at T451 and PAK2 phosphorylation at S141, respectively (Fig. 7). These results were further confirmed by immunofluorescence analysis (Fig. S6). In the *in vivo* experiment, PKAIIa phosphorylation was detected in the control and PFDoA-treated rats. Moreover, PKAIIa phosphorylation significantly increased following 0.02 mg/kg/d PFDoA exposure (Fig. 5).

4. Discussion

Phosphorylation analysis of the primary testis, in contrast to immortalized cell lines, best represents events that occur in the basal physiological state even though tissues often contain heterogeneous populations of cells. To understand the link between protein phosphorylation and testicular activity, it is necessary to determine the characteristics of testicular protein

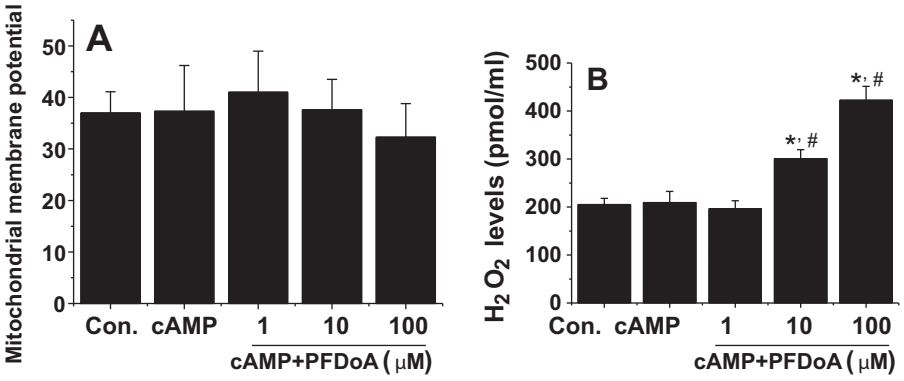

Fig. 6. Effect of PFDoA exposure on (A) mitochondrial membrane potential and (B) H_2O_2 level in primary Leydig cells. Data are presented as means ± SEM ($n = 4$) from four independent experiments. * indicates significant difference from untreated controls ($p < 0.05$), # indicates significant difference from the cAMP group ($p < 0.05$).

phosphorylation profiles. In the current study, we first identified the testicular phosphorylation profile in normal and PFDoA-exposed rats with TiO_2 and IMAC phosphopeptide enrichment, outlined the critical molecular pathways (*e.g.* MAPK signaling) in testicular activity, and discovered 937 novel phosphorylated sites in testicular proteins. Our findings are the first to feature protein phosphorylation in testes in order to understand their role in testicular function and PFDoA toxic effects.

4.1. Roles of kinases in testicular protein phosphorylation

The Ser/Thr protein kinases are defined as proline-directed, basophilic, or acidiphilic based on their preferred substrate sequences (Beausoleil et al., 2006). To better understand the classes of kinases involved in these positional effects, we categorized all localized phosphorylation sites into these three general sequence types. In the control rats, we found that proline-directed

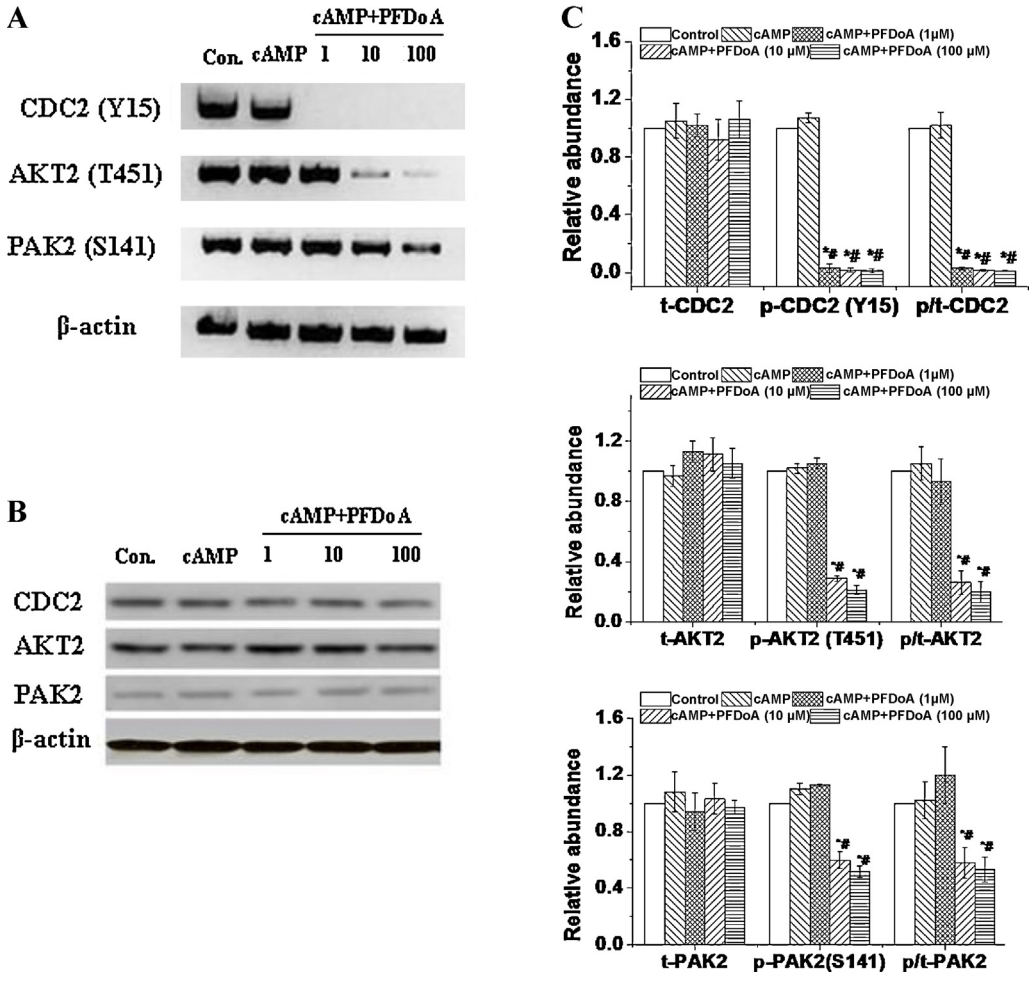

Fig. 7. Effect of PFDoA exposure on proteins and their phosphorylated levels for CDC2 phosphorylation (Y15), AKT2 phosphorylation (T451), and PAK2 phosphorylation (S141) in primary Leydig cells. (A) Immunoblots of phosphorylated protein; (B) immunoblots of proteins; (C) quantification of phosphorylated protein levels. Data are presented as means ± SEM ($n = 3$) from three independent experiments. * indicates significant difference from untreated controls ($p < 0.05$), # indicates significant difference from the cAMP group ($p < 0.05$).

phosphorylation was in greatest abundance, while acidic motifs were lowest. We postulated, therefore, that relative to the other two phosphorylation types, proline-directed phosphorylation may be dominant for testicular function. Indeed, another study also demonstrated that proline-directed phosphorylation plays an important role in spermatogenesis and cell cycles (Jha et al., 2006). Serine/threonine phosphorylation is a classic proline-directed phosphorylation and is essential for regulation of cellular processes such as cell proliferation and differentiation. In testes, the role of serine/threonine protein kinase A (PKA) in sperm capacitation and testosterone synthesis has been well established. Null mutants of the testis-specific PKA catalytic subunit C2α are infertile and display capacitation-related defects such as a lack in tyrosine phosphorylation increase (Nolan et al., 2004). Moreover, proline-directed kinases such as CDK2 and proline-directed phosphatases such as CDC14 are crucial in spermatogenesis and sperm capacitation (Viera et al., 2009). Our findings provide an explanation for why proline-directed phosphorylation is highly correlated with testicular function. After PFDoA exposure, we observed that acid-directed phosphorylation exhibited at least a four-fold increase compared to the control, suggesting that acid-directed phosphorylation may participate in PFDoA testicular toxicity. At the highest dose, proline-directed phosphorylation decreased by 60% that of the control. Considering PKA activity is controlled by proline-directed phosphorylation and is necessary for testosterone production, the decreased testosterone from the same PFDoA-exposed rats in previously published results may be influenced by decreased proline-directed phosphorylation. We previously observed sperm apoptosis in rat testes following acute and chronic PFDoA exposure (Shi et al., 2009, 2010a,b). Thus, the adverse effect of PFDoA on sperm activity may be associated with proline-directed kinases.

4.2. Phosphorylation at particular amino acids in testicular proteins

In control rat testis, 89.9% of phosphorylated peptides were singly phosphorylated, suggesting that testicular function is largely regulated by single phosphorylation. Moreover, of all phosphorylated amino acids, 87.6% and 11.5% were identified as Ser and Thr in control rat testis, respectively. Thus, Ser and Thr phosphorylation would appear important for maintaining testicular function. For example, testis-specific kinases include the recently described Ser/Thr kinases TSSK 1, 2, and 3 (Beausoleil et al., 2006). This kinase family may participate in sperm differentiation and/or subsequent sperm function during maturation, capacitation, and fertilization. Thus, it is important to examine the detailed role of Ser/Thr kinases activity in sperm synthesis. In addition, HSP90β is a chaperone for several proteins and is known to participate in some aspects of spermatogenesis. However, little is known about the action mechanism of HSP90β during spermatogenesis (Saribek et al., 2006). We showed that HSP90β was phosphorylated at a novel site and known site, Ser-365 and Ser-255, respectively. This provides a basis for further study of HSP90β's role in spermatogenesis.

4.3. The MAPK pathway and significance of CDC2 in testicular function

The MAPK pathway is involved in testicular functions, including hormone synthesis, cell communication, spermatogenesis, germ cell cycle progression, and germ cell apoptosis (Almog and Naor, 2010). However, detailed understanding of the action of these pathways is lacking.

The AKT1 gene is involved in germ cell survival and proliferation (Chen et al., 2001). Of interest, homozygous deletion of the ubiquitously expressed AKT1 has led to spontaneous apoptosis and attenuation of spermatogenesis in mice testes (Chen et al., 2001). Moreover, AKT1 is implicated as a downstream target in a PI3K-dependent signal transduction pathway in neonatal rat Sertoli cells and its function is dependent on phosphorylation at Thr-308 and Ser-473 (Meroni et al., 2002). Through analysis of the regulatory network of the MAPK pathway, it seems reasonable to assume that AKT1-mediated phosphorylation may be involved in germ cell development and AKT1 may be associated with spermatogenesis in rat testes.

Stathmin has recently been shown to bind tubulin heterodimers and destabilize microtubules by promoting depolymerization, although the molecular mechanisms of this function remain unclear (Cassimeris, 1999). Our analysis of the regulatory network of MAPK, MAPK13, and MAPK11 showed that it may be possible to phosphorylate stathmin. Such results are useful for our understanding of the action mechanism of stathmin. In the MAPK pathway, the function of many proteins is likely related to CDC2, suggesting that CDC2 may play a general role as an intracellular integrator of diverse cell signaling pathways (Woo and Poon, 2003). Strong evidence indicates that CDC2 participates in different stages of spermatogenesis (Alekseev et al., 2009). In the network of CDC2 interacting proteins, it would be interesting to investigate the role of novel phosphorylation site (T853) from MAP4 in mediating CDC2 functions in future studies. In mammals, CDC2 activity in pachytene spermatocytes is required for G2/M transition in prophase I (Soung et al., 2009). Moreover, CDC2 sustains a balance between sperm production and apoptosis (Alekseev et al., 2009). Further research involving CDC2 has shown that phosphorylation is crucial for germ cell differentiation (Rose et al., 2008). However, the exact mechanism for the function of CDC2 during sperm development is uncertain. Our findings provide information for further study of the interaction of CDC2 with spermatogenesis-related proteins and participation in sperm development regulation.

4.4. The significance of protein phosphorylation in PFDoA toxicity

In this study, PFDoA exposure resulted in significant decreases in phosphorylation levels of most proteins, showing that PFDoA played an inhibition role in protein phosphorylation. Among proteins which showed significant changes at the phosphorylation level, the function of some (*e.g.* vimentin, TPX2 and map1b) were associated with microtube assembly. Moreover, their phosphorylation levels exhibited marked reductions following PFDoA exposure. These results suggest PFDoA may disrupt the cytoskeleton organization in testicular cells.

Vimentin is an intermediate filament protein expressed in Sertoli cells in immature and adult rat testes (Devkota et al., 2010). Phosphorylation of this protein plays an important role in the cytoskeletal framework and normal cell morphology (Devkota et al., 2010). Perfluorononanoic acid, a homolog of PFDoA, disrupts Sertoli cell shape in rat testes without affecting the expression of vimentin mRNA or protein (Shi et al., 2010b). Moreover, PFDoA also causes ultra-structural changes in Sertoli cells in rats (Shi et al., 2009). In this present study, vimentin phosphorylation was markedly diminished by all doses of PFDoA. Thus, we hypothesize that decreased vimentin phosphorylation may contribute to the change in Sertoli cell morphology in PFDoA-exposed testes.

Normal sperm function is dependent on sperm motility, which is related to outer dense fiber proteins (ODFs) and A-kinase anchor protein (AKAP). As specialized cytoskeletal elements of the mammalian sperm tail, ODFs are conserved among various mammals, suggesting a critical function in testes (Mariappa et al., 2006). While ODF2 mutation can lead to infertility in mice, few reports exist on ODF phosphorylation in sperm. As PFDoA exposure resulted in decreased phosphorylation of ODF at various Ser residues, particularly the 86-fold reduction for the phosphorylated peptide of ILASSCCSpSpNILGSVNVCGFEPDQVK at the highest dose,

we predicted that PFDoA may produce adverse effects on sperm function *via* changes in ODF phosphorylation. Both AKAP4 and AKAP3 are major fibrous sheath proteins in sperm and are important for fibrous sheath assembly, with AKAP4 phosphorylation also associated with sperm motility (Mariappa et al., 2006; Carr and Newell, 2007). In the current study, PFDoA decreased the levels of AKAP4 and AKAP3 phosphorylation in rat testes, providing further evidence that PFDoA may disrupt the structure of the sperm fibrous sheath, leading to abnormal sperm motility. Considering that normal sperm motility is essential for fertilization, these results strongly suggest that PFDoA may disrupt sperm activity and function. Thus, caution should be considered regarding human exposure to PFDoA. In addition, we found some new sites in AKAP3, AKAP4, and ODF proteins involved in sperm production and testicular cell morphology, suggesting they may play an important role in mediating related protein functions. Although the functions of these sites were not investigated, this finding provides an avenue to explore the role of the corresponding proteins in testicular activity and PFDoA toxicity effects. Considering the conserved feature of phosphorylated sites across mammalian species, these novel sites will also offer additional information for studying human reproductive activity.

4.5. Leydig cells' dysfunction in PFDoA exposure

In this current *in vitro* experiment, we firstly observed the elevation of mitochondrial H_2O_2 in primary Leydig cells after PFDoA treatment. Considering H_2O_2 is a primary oxidative stress molecule, oxidative stress may be an important source for the function inhibition of Leydig cells. Previous research has shown that H_2O_2 treatment induces G2/M phase arrest of HLE B-3 cells (Seomun et al., 2005). In addition, CDC2 phosphorylated at Tyr15 is a key factor in G2/M transition (Li et al., 2009). In this study, CDC2 phosphorylation levels were significantly inhibited by all doses of PFDoA in primary Leydig cells. Therefore, we speculated that H_2O_2 may affect Leydig cell function by CDC2 phosphorylation at Tyr15. This indicates that oxidative stress and cell cycle disruption may participate in PFDoA-mediated testosterone inhibition. Both AKT2 and PAK2 may regulate mitochondrial function by supporting intact membrane structure (Bijur and Jope, 2003; Jung et al., 2008). Chronic PFDoA exposure led to mitochondrial structure disruption in the Leydig cells of rats (Shi et al., 2009, 2010a,b). Based on these results, AKT2 and PAK2 phosphorylation inhibition may induce PFDoA mitochondrial toxicity in Leydig cells. Research has shown that PKAIIa is a regulator for mitochondrial function and exhibits a special role in mitochondrial integrity and membrane potential (Erlichman et al., 1999). In our *in vivo* experiment, PFDoA treatment possibly caused PKAIIa (Ser96) phosphorylation, suggesting PKAIIa participation in PFDoA mitochondrial toxicity in testes. However, the mitochondrial membrane potential remained stable in Leydig cells upon PFDoA exposure, implying that complex mechanisms were involved in the toxic effect of PFDoA on Leydig cells. Combining the *in vivo* and *in vitro* experiments, oxidative stress and abnormal protein phosphorylation in mitochondrial function may contribute to the toxic effect of PFDoA on testes. In particular, CDC2 may be a sensitive factor in PFDoA testicular toxicity as no CDC2 phosphorylation at Tyr15 in PFDoA-treated Leydig cells was observed.

Generally, there should be at least ten animals per group while performing experiments related to reproductive toxicology. In this study, only six animals each group were tested *in vivo*. This may make interpretations difficult when effects exist but are not evident. However, combining the *in vitro* experiment, this study is beneficial to selecting dosage, crucial molecular indicators and potential molecular targets for future PFDoA toxicological study.

5. Conclusion

By combining TiO_2 and IMAC methods, our study is the first to describe the phosphorylation profile of rat testicular proteins in control and PFDoA exposure groups and to reveal the molecular network at the post-translational level in testicular function. The functions of most phosphorylated proteins were related to spermatogenesis and sperm function. Moreover, PFDoA exposure led to a significant increase in the acidic motif rate and changes in protein phosphorylation levels in rat testes. In addition, 937 novel phosphorylated sites in testicular proteins were identified in our study and CDC2 may be a key factor for inducing PFDoA testicular toxicity. Taken together, these data provide a unique and detailed insight into the roles of phosphorylation in testicular function.

Conflict of interest

The authors declare that there are no conflicts of interest.

Acknowledgment

This work was supported by the National Key Basic Research Program of China (973 Program: 2013CB945204) and the National Natural Science Foundation of China (Grant 31025006).

Appendix A. Supplementary data

Supplementary data associated with this article can be found, in the online version, at http://dx.doi.org/10.1016/j.toxlet.2013.06.219.

References

Adinolfi, E., Callegari, M.G., Ferrari, D., Bolognesi, C., Minelli, M., Wieckowski, M.R., et al., 2005. Basal activation of the P2X7 ATP receptor elevates mitochondrial calcium and potential, increases cellular ATP levels, and promotes serum-independent growth. Molecular Biology of the Cell 16, 3260–3272.

Alekseev, O.M., Richardson, R.T., O'Rand, M.G., 2009. Linker histones stimulate HSPA2 ATPase activity through NASP binding and inhibit CDC2/Cyclin B1 complex formation during meiosis in the mouse. Biology of Reproduction 81, 739–748.

Almog, T., Naor, Z., 2010. The role of mitogen activated protein kinase (MAPK) in sperm functions. Molecular and Cellular Endocrinology 314, 239–243.

Andric, S.A., Janjic, M.M., Stojkov, N.J., Kostic, T.S., 2007. Protein kinase G-mediated stimulation of basal Leydig cell steroidogenesis. American Journal of Physiology: Endocrinology and Metabolism 293, E1399–E1408.

Beausoleil, S.A., Villen, J., Gerber, S.A., Rush, J., Gygi, S.P., 2006. A probability-based approach for high-throughput protein phosphorylation analysis and site localization. Nature Biotechnology 24, 1285–1292.

Bijur, G.N., Jope, R.S., 2003. Rapid accumulation of Akt in mitochondria following phosphatidylinositol 3-kinase activation. Journal of Neurochemistry 87, 1427–1435.

Carr, D.W., Newell, A.E., 2007. The role of A-kinase anchoring proteins (AKaps) in regulating sperm function. Society of Reproduction and Fertility Supplement 63, 135–141.

Cassimeris, L., 1999. Accessory protein regulation of microtubule dynamics throughout the cell cycle. Current Opinion in Cell Biology 11, 134–141.

Chen, W.S., Xu, P.Z., Gottlob, K., Chen, M.L., Sokol, K., Shiyanova, T., et al., 2001. Growth retardation and increased apoptosis in mice with homozygous disruption of the Akt1 gene. Genes and Development 15, 2203–2208.

Cui, Z., Chen, X., Lu, B., Park, S.K., Xu, T., et al., 2009. Preliminary quantitative profile of differential protein expression between rat L6 myoblasts and myotubes by stable isotope labeling with amino acids in cell culture. Proteomics 9, 1274–1292.

Devkota, B., Sasaki, M., Matsui, M., Takahashi, K., Matsuzaki, S., Koseki, T., et al., 2010. Effects of scrotal insulation and pathological lesions on alpha-Smooth Muscle Actin (SMA) and vimentin in the bull testes. Journal of Reproduction and Development 56, 187–190.

Eng, J.K., McCormack, A., Yates III, J.R., 1994. An approach to correlate tandem mass spectral data of peptides with amino acid sequences in a protein database. Journal of the American Society for Mass Spectrometry 5, 976–989.

Erlichman, J., Gutierrez-Juarez, R., Zucker, S., Mei, X., Orr, G.A., 1999. Developmental expression of the protein kinase C substrate/binding protein (clone 72/SSeCKS) in rat testis identification as a scaffolding protein containing an A-kinase-anchoring domain which is expressed during late-stage spermatogenesis. European Journal of Biochemistry 263, 797–805.

Evaul, K., Hammes, S.R., 2008. Cross-talk between G protein-coupled and epidermal growth factor receptors regulates gonadotropin-mediated steroidogenesis in Leydig cells. Journal of Biological Chemistry 283, 27525–27533.

Ficarro, S., Chertihin, O., Westbrook, V.A., White, F., Jayes, F., Kalab, P., et al., 2003. Phosphoproteome analysis of capacitated human sperm. Evidence of tyrosine phosphorylation of a kinase-anchoring protein 3 and valosin-containing protein/p97 during capacitation. Journal of Biological Chemistry 278, 11579–11589.

Guruge, K.S., Taniyasu, S., Yamashita, N., Wijeratna, S., Mohotti, K.M., Seneviratne, H.R., et al., 2005. Perfluorinated organic compounds in human blood serum and seminal plasma: a study of urban and rural tea worker populations in Sri Lanka. Journal of Environmental Monitoring 7, 371–377.

Hojlund, K., Bowen, B.P., Hwang, H., Flynn, C.R., Madireddy, L., Geetha, T., et al., 2009. In vivo phosphoproteome of human skeletal muscle revealed by phosphopeptide enrichment and HPLC–ESI-MS/MS. Journal of Proteome Research 8, 4954–4965.

Hou, J., Cui, Z., Xie, Z., Xue, P., Wu, P., Chen, X., et al., 2010. Phosphoproteome analysis of rat L6 myotubes using reversed-phase C18 prefractionation and titanium dioxide enrichment. Journal of Proteome Research 9, 777–788.

Jha, K.N., Salicioni, A.M., Arcelay, E., Chertihin, O., Kumari, S., Herr, J.C., et al., 2006. Evidence for the involvement of proline-directed serine/threonine phosphorylation in sperm capacitation. Molecular Human Reproduction 12, 781–789.

Jung, J.H., Pendergast, A.M., Zipfel, P.A., Traugh, J.A., 2008. Phosphorylation of c-Abl by protein kinase Pak2 regulates differential binding of ABI2 and CRK. Biochemistry 47, 1094–1104.

Kennedy Jr., G.L., Butenhoff, J.L., Olsen, G.W., O'Connor, J.C., Seacat, A.M., Perkins, R.G., et al., 2004. The toxicology of perfluorooctanoate. Critical Reviews in Toxicology 34, 351–384.

Klinefelter, G.R., Hall, P.F., Ewing, L.L., 1987. Effect of luteinizing hormone deprivation in situ on steroidogenesis of rat Leydig cells purified by a multistep procedure. Biology of Reproduction 36, 769–783.

Li, R., Tang, X.L., Miao, S.Y., Zong, S.D., Wang, L.F., 2009. Regulation of the G2/M phase of the cell cycle by sperm associated antigen 8 (SPAG8) protein. Cell Biochemistry and Function 27, 264–268.

Linding, R., Jensen, L.J., Pasculescu, A., Olhovsky, M., Colwill, K., Bork, P., et al., 2008. NetworKIN: a resource for exploring cellular phosphorylation networks. Nucleic Acids Research 36, D695–D699.

Maere, S., Heymans, K., Kuiper, M., 2005. BiNGO: a Cytoscape plugin to assess overrepresentation of gene ontology categories in biological networks. Bioinformatics 21, 3448–3449.

Mariappa, D., Siva, A.B., Shivaji, S., Seshagiri, P.B., 2006. Tyrphostin-A47 inhibitable tyrosine phosphorylation of flagellar proteins is associated with distinct alteration of motility pattern in hamster spermatozoa. Molecular Reproduction and Development 73, 215–225.

Meroni, S.B., Riera, M.F., Pellizzari, E.H., Cigorraga, S.B., 2002. Regulation of rat Sertoli cell function by FSH: possible role of phosphatidylinositol 3-kinase/protein kinase B pathway. Journal of Endocrinology 174, 195–204.

Mondillo, C., Pagotto, R.M., Piotrkowski, B., Reche, C.G., Patrignani, Z.J., Cymeryng, C.B., et al., 2009. Involvement of nitric oxide synthase in the mechanism of histamine-induced inhibition of Leydig cell steroidogenesis via histamine receptor subtypes in Sprague-Dawley rats. Biology of Reproduction 80, 144–152.

Nolan, M.A., Babcock, D.F., Wennemuth, G., Brown, W., Burton, K.A., McKnight, G.S., 2004. Sperm-specific protein kinase A catalytic subunit Calpha2 orchestrates cAMP signaling for male fertility. Proceedings of the National Academy of Sciences of the United States of America 101, 13483–13488.

Olsen, J.V., Blagoev, B., Gnad, F., Macek, B., Kumar, C., Mortensen, P., et al., 2006. Global, in vivo, and site-specific phosphorylation dynamics in signaling networks. Cell 127, 635–648.

Rose, K.L., Li, A., Zalenskaya, I., Zhang, Y., Unni, E., Hodgson, K.C., et al., 2008. C-terminal phosphorylation of murine testis-specific histone H1t in elongating spermatids. Journal of Proteome Research 7, 4070–4078.

Saribek, B., Jin, Y., Saigo, M., Eto, K., Abe, S., 2006. HSP90b is involved in signaling prolactin-induced apoptosis in newt testis. Biochemical and Biophysical Research Communications 349, 1190–1197.

Schwartz, D., Gygi, S.P., 2005. An iterative statistical approach to the identification of protein phosphorylation motifs from large-scale data sets. Nature Biotechnology 23, 1391–1398.

Seomun, Y., Kim, J.T., Kim, H.S., Park, J.Y., Joo, C.K., 2005. Induction of p21Cip1-mediated G2/M arrest in H_2O_2-treated lens epithelial cells. Molecular Vision 11, 764–774.

Shi, Z., Ding, L., Zhang, H., Feng, Y., Xu, M., Dai, J., 2009. Chronic exposure to perfluorododecanoic acid disrupts testicular steroidogenesis and the expression of related genes in male rats. Toxicology Letters 188, 192–200.

Shi, Z., Feng, Y., Wang, J., Zhang, H., Ding, L., Dai, J., 2010a. Perfluorododecanoic acid-induced steroidogenic inhibition is associated with steroidogenic acute regulatory protein and reactive oxygen species in cAMP-stimulated Leydig cells. Toxicological Sciences 114, 285–294.

Shi, Z., Zhang, H., Ding, L., Feng, Y., Wang, J., Dai, J., 2010b. Proteomic analysis for testis of rats chronically exposed to perfluorododecanoic acid. Toxicology Letters 192, 179–188.

Soung, N.K., Park, J.E., Yu, L.R., Lee, K.H., Lee, J.M., Bang, J.K., et al., 2009. Plk1-dependent and -independent roles of an ODF2 splice variant, hCenexin1, at the centrosome of somatic cells. Developmental Cell 16, 539–550.

Tao, L., Kannan, K., Wong, C.M., Arcaro, K.F., Butenhoff, J.L., 2008. Perfluorinated compounds in human milk from Massachusetts, U.S.A. Environmental Science and Technology 42, 3096–3101.

Urner, F., Sakkas, D., 2003. Protein phosphorylation in mammalian spermatozoa. Reproduction 125, 17–26.

Van de Vijver, K.I., Holsbeek, L., Das, K., Blust, R., Joiris, C., De, C.W., 2007. Occurrence of perfluorooctane sulfonate and other perfluorinated alkylated substances in harbor porpoises from the Black Sea. Environmental Science and Technology 41, 315–320.

Viera, A., Rufas, J.S., Martinez, I., Barbero, J.L., Ortega, S., Suja, J.A., 2009. CDK2 is required for proper homologous pairing, recombination and sex-body formation during male mouse meiosis. Journal of Cell Science 122, 2149–2159.

Woo, R.A., Poon, R.Y., 2003. Cyclin-dependent kinases and S phase control in mammalian cells. Cell Cycle 2, 316–324.

Wu, J., Shakey, Q., Liu, W., Schuller, A., Follettie, M.T., 2007. Global profiling of phosphopeptides by titania affinity enrichment. Journal of Proteome Research 6, 4684–4689.

Yang, Y., Sharma, R., Cheng, J.Z., Saini, M.K., Ansari, N.H., Andley, U.P., et al., 2002. Protection of HLE B-3 cells against hydrogen peroxide- and naphthalene-induced lipid peroxidation and apoptosis by transfection with hGSTA1 and hGSTA2. Investigative Ophthalmology and Visual Science 43, 434–445.